Journal of Solid State Chemistry **148,** 425–432 (1999)
Article ID jssc.1999.8471, available online at http://www.idealibrary.com on IDEAL®

Complex Three-Dimensional $[Au_3In_5]$ Polyanions in $Ln_2Au_3In_5$ (Ln = Ce, Pr, Nd, Sm)

Yaroslav V. Galadzhun,*,[1] Rolf-Dieter Hoffmann,* Rainer Pöttgen,* and Martin Adam†

*Anorganisch-Chemisches Institut, Universität Münster, Wilhelm-Klemm-Strasse 8, D-48149 Münster; and
†Nonius GmbH, P.O. Box 10 10 30, D-42648 Solingen, Germany
E-mail: pottgen@uni-muenster.de, adam@nonius.nl

Received May 11, 1999; in revised form July 28, 1999; accepted August 10, 1999

The four isotypic title compounds were prepared from the elements by reactions in an arc-melting furnace and subsequent annealing in sealed silica tubes at 970 K. The structure of the cerium compound was solved from single crystal X-ray diffractometer data: $Pmn2_1$, oP80, $a = 465.27(8)$ pm, $b = 5348.3(9)$ pm, $c = 740.5(1)$ pm, $R1 = 0.0735$, 5552 F^2 values, 243 variables, and BASF = 0.48(2). The structure of $Ce_2Au_3In_5$ is composed of a complex three-dimensional $[Au_3In_5]$ polyanion with a large variety of Au–In and In–In bonds. The cerium atoms are embedded in distorted pentagonal and hexagonal channels within this polyanion. The crystal chemical relationship of the $Ce_2Au_3In_5$ structure with the structures of the related stannides $Y_2Rh_3Sn_5$ (oC40, $Cmc2_1$) and $Yb_2Pt_3Sn_5$ (oP40, $Pnma$) is discussed. The differences in these three structure types result from a different ordering of the transition metal and tin(indium) atoms within the polyanionic network. Temperature-dependent magnetic susceptibility measurements of $Ce_2Au_3In_5$ show modified Curie–Weiss behavior with $\chi_0 = 5.2\times10^{-9}$ m^3/mol, $\Theta = -16(1)$ K, and $\mu_{exp} = 2.51(2)$ μ_B/Ce, indicating trivalent cerium. No magnetic ordering could be observed down to 2 K. © 1999 Academic Press

Key Words: **intermetallic rare earth compounds; crystal structure; superstructure; indium compounds.**

INTRODUCTION

Ternary rare earth–transition metal (T)–indides have intensively been investigated in recent years with respect to their crystal structures (1) and physical properties (2). Most work has been done on those compounds with iron, cobalt, nickel, and copper as transition metal component. Structural elements of these indides are two- and three-dimensional transition metal–indium polyanions, where the rare earth atoms separate polyanionic layers or they are embedded in channels of a three-dimensional $[T_xIn_y]$ network. Recently, a brief review on the various structure types of rare earth–3d transition metal–indium compounds was given by Kalychak (3). Some notable structures with the 3d transition metals are $LaNi_3In_6$ (4), $Ce_4Ni_7In_8$ (5), $Ho_{10}Ni_9In_{20}$ (6), $CeCu_{4.38}In_{1.62}$ (7), $Sm_2Co_9In_3$ (8), $CeNiIn_4$ (9), and $Nd_5Ni_6In_{11}$ (10).

With 4d and 5d transition metals, only the equiatomic compounds LnTIn have systematically been investigated (1, 2), while little is known about the phase diagrams of these ternary systems. For the last five years we have been enforcing a more systematic investigation of these systems and we were successful in preparing the new indides $EuAg_4In_8$ (11), $YbAg_2In_4$ (12), $LnPtIn_3$ (Ln = La, Ce, Pr, Nd, Sm), $LaPtIn_4$ (13), $EuPdIn_2$, $YbPdIn_2$, and $YbAuIn_2$ (14). In the present paper we report on the new isotypic indium compounds $Ln_2Au_3In_5$ (Ln = Ce, Pr, Nd, Sm). These compounds crystallize with a peculiar structure type with a complex three-dimensional $[Au_3In_5]$ polyanion. The $Ln_2Au_3In_5$ structure shares great similarities with the structures of $Y_2Rh_3Sn_5$ (15) and $Yb_2Pt_3Sn_5$ (16).

EXPERIMENTAL

Starting materials for the preparation of $Ln_2Au_3In_5$ (Ln = Ce, Pr, Nd, Sm) were ingots of the rare earth elements (Johnson Matthey and Kelpin), gold wire (Degussa, ∅ 1 mm), and indium tear drops (Johnson Matthey), all with stated purities greater than 99.9%. The moisture-sensitive large rare earth metal ingots were cut into small pieces under paraffin oil which was subsequently washed off with n-hexane. The paraffin oil and n-hexane had been previously dried over sodium wire. The cut-up rare earth ingots (about 200 mg) were arc-melted to buttons in a first step and kept in Schlenk tubes. This premelting procedure prevents a shattering of the buttons during the next reaction step.

In the second step, the rare earth metal buttons were mixed with gold wire and indium tear drops in the ideal 2 : 3 : 5 atomic ratio and arc-melted under an argon pressure

[1]Permanent address: Inorganic Chemistry Department, Ivan Franko Lviv State University, Kyryla and Mephodiya Street 6, 290005 Lviv, Ukraine.

0022-4596/99 $30.00

of about 600 mbar in a miniaturized arc-melting apparatus. The argon was purified over molecular sieves and titanium sponge (900 K). Details about the arc-melting apparatus are given in reference (17). The resulting buttons were remelted at least three times to ensure homogeneity. The total weight losses after the melting procedures were less than 0.5 wt%. The compact polycrystalline products were subsequently sealed in evacuated silica tubes and annealed at 970 K for 3 weeks.

The samples were analyzed further by metallography. The microstructures of polished samples were left unetched and were examined with a Leica 420 I scanning electron microscope in backscattering mode. The compositions were determined by energy dispersive X-ray analyses (EDX) with CeO_2, elemental Au, and InAs as standards. The composition of 22 at% Ce, 28 at% Au, and 50 at% In matched within the error limits the ideal formula, $Ce_2Au_3In_5$, derived by the structure determination.

Powders and single crystals of the investigated indium compounds show a light gray color and are stable in air. No decomposition was observed after several months. Single crystals had platelet-like shape and exhibited silvery metallic luster.

Guinier powder patterns of the samples were recorded at room temperature with Cu$K\alpha_1$ radiation using α-quartz ($a = 491.30$ pm, $c = 540.46$ pm) as an internal standard. The orthorhombic lattice constants (see Table 1) were obtained from least-squares fits of the Guinier data. To assure correct indexing, the observed patterns were compared with calculated ones (18), taking the atomic positions from the structure refinement. For $Ce_2Au_3In_5$ the lattice constants determined from the powder pattern and those from different single crystals agreed well.

Single crystal intensity data were collected at room temperature by use of a Nonius KappaCCD diffractometer with graphite monochromatized Mo$K\alpha$ radiation (71.073 pm, rotating anode). Data integration was performed using Denzo-SMN (19, 20). An empirical absorption correction was applied on the basis of the Sortav procedure (21).

The magnetic properties of $Ce_2Au_3In_5$ were determined by use of an MPMS SQUID magnetometer (Quantum Design, Inc.) in the temperature range 2–300 K with magnetic flux densities up to 3 T.

RESULTS AND DISCUSSION

Structure Determination

Small, platelet-like single crystals of $Ce_2Au_3In_5$ were isolated from the annealed sample and examined by use of a Weissenberg camera. Crystals which showed high-quality Laue photographs were further characterized by their reciprocal layers *hk*0 and *hk*1. The film data were in good agreement with the orthorhombic unit cell listed in Table 1, and the extinction conditions were compatible with space group $Pmn2_1$. All relevant crystallographic data and experimental details for the data collection are listed in Table 2.

TABLE 1
Lattice Constants of the Orthorhombic Compounds $Ln_2Au_3In_5$ (Ln = Ce, Pr, Nd, Sm)

Compound	a (pm)	b (pm)	c (pm)	V (nm^3)
$Ce_2Au_3In_5$	465.27(8)	5348.3(9)	740.5(1)	1.8427
$Pr_2Au_3In_5$	461.81(6)	5350.7(9)	742.2(1)	1.8340
$Nd_2Au_3In_5$	459.98(6)	5338.2(8)	740.7(1)	1.8188
$Sm_2Au_3In_5$	456.40(7)	5332.5(9)	739.4(1)	1.7995

Note. Standard deviations in the positions of the last significant digits are given in parentheses.

The assignment of the correct space group was the key to the solution of the structure of $Ce_2Au_3In_5$. The reciprocal lattice was clearly primitive, but with systematically occuring strong and weak reflections. The strong reflections comply with space group *Cmcm* ($a = 465.3$ pm, $b' = b/2 = 2674.2$ pm, $c = 740.5$ pm, $V = 0.921$ nm^3). The space group *Cmcm* is the common supergroup found for $Y_2Rh_3Sn_5$ ($Cmc2_1$) (15) and $Yb_2Pt_3Sn_5$ (*Pnma*) (16) as outlined in Fig. 1. Therefore, a first structure solution using direct methods with SHELXS-97 (22) was carried out for the subcell. This resulted in two cerium sites and eight mixed gold (indium) sites with $R1 = 0.14$ and 676 F^2 values. Two

TABLE 2
Crystal Data and Structure Refinement for $Ce_2Au_3In_5$

Empirical formula	$Ce_2Au_3In_5$
Molar mass (g/mol)	1445.24
Space group, Z	$Pmn2_1$ (No. 31), 8
Lattice constants	see Table 1
Calculated density (g/cm^3)	10.42
Crystal size (μm^3)	$15 \times 25 \times 40$
Transmission ratio (max/min)	2.09
Absorption coefficient (mm^{-1})	69.4
F(000)	4784
Detector distance (mm)	64.4
Oscillation angle	0.53°
Total no. of frames	1821
Total exposure time (h)	94.5
θ range for data collection	2° to 33°
Range in *hkl*	± 7, ± 80, ± 11
Total no. of reflections	26153
Independent reflections	5552 ($R_{int} = 0.1264$)
Reflections with $I > 2\sigma(I)$	4053 ($R_{sigma} = 0.0881$)
Data/restraints/parameters	5552/0/243
Goodness-of-fit on F^2	1.112
Final R indices [$I > 2\sigma(I)$]	$R1 = 0.0588$; $wR2 = 0.1741$
R indices (all data)	$R1 = 0.0735$, $wR2 = 0.1895$
Refined BASF	0.48(2)
Extinction coefficient	0.00045(6)
Largest diff. peak and hole	3.72 and -3.77 e/Å^3

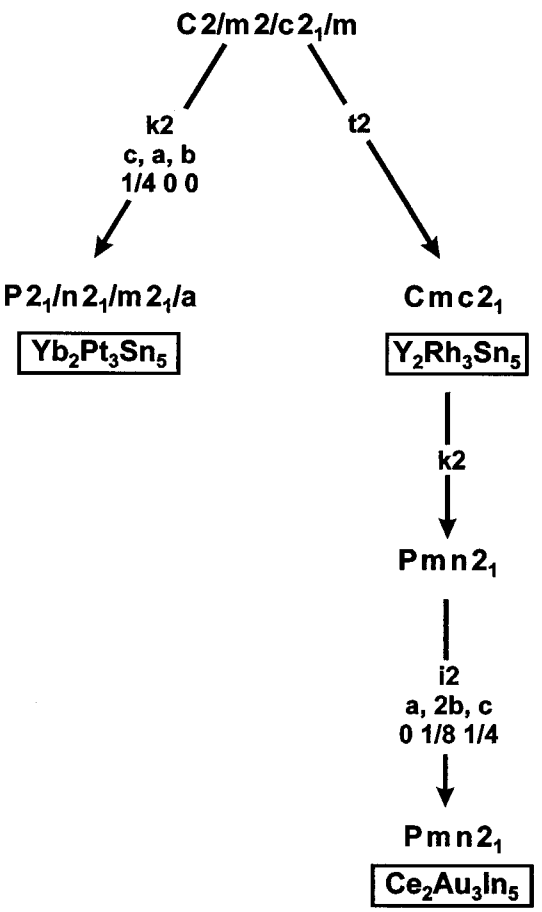

FIG. 1. Group–subgroup relationship (33, 34) for the structures of $Y_2Rh_3Sn_5$, $Yb_2Pt_3Sn_5$, and $Ce_2Au_3In_5$. The indices of the *klassengleiche* (k), isomorphic (i), and *translationengleiche* (t) transitions, the shifts in origin, and the unit cell transformations are given.

steps of symmetry reduction are necessary to get the space group of the superstructure, i.e., decentering ($k2$) and doubling of the b axis ($i2$). This led unambiguously to space group $Pmn2_1$ (Fig. 1). The starting atomic parameters for the correct space group $Pmn2_1$ were deduced from an automatic interpretation of direct methods with SHELXS-97 (22) and assigned to cerium, gold, and indium sites according to the precalculated parameters derived from the subcell refinement. The structure was subsequently refined using SHELXL-97 (23) (full-matrix least-squares on F^2) with anisotropic atomic displacement parameters for all atoms with $R1 = 0.0588$. Additionally, we observed twinning by inversion. This could be expected by the *translationengleiche* symmetry reduction of index 2 in going from the idealized subcell structure of space group *Cmcm* to the first ordered variant $Y_2Rh_3Sn_5$ (15) (Fig. 1). The twin ratio was determined to be 1:0.92. The refinement converged rather smoothly, but no damping was necessary. A final difference Fourier synthesis revealed no significant residual peaks (see Table 2). The final $wR2$ of 0.1741 is elevated due to statistical reasons; F^2-based $wR2$ values are about twice as large as conventinal residuals (based on F), and the many weak superstructure reflections additionally increase $wR2$ (Table 2).

As a further check for the correct site assignments, the occupancy parameters of the gold and indium sites were varied in a separate series of least-squares cycles, while the occupancies of the cerium atoms were held fixed at their ideal values. The occupancy parameters varied between $94 \pm 2\%$ and $106 \pm 2\%$, indicating that gold and indium

TABLE 3
Atomic Coordinates and Isotropic Displacement Parameters (pm^2) of $Ce_2Au_3In_5$ (All Positions Occupy the Site 2*a* of Space Group $Pmn2_1$)

Atom	x	y	z	U_{eq}
Ce1	0	0.11547(5)	0.9021(3)	225(4)
Ce2	0	0.13424(5)	0.4008(3)	212(4)
Ce3	0	0.28853(5)	0.4342(3)	247(5)
Ce4	0	0.46181(6)	0.9379(3)	252(5)
Ce5	0	0.61566(5)	0.9706(3)	226(4)
Ce6	0	0.63459(5)	0.4696(3)	235(4)
Ce7	0	0.78788(5)	0.4335(3)	230(5)
Ce8	0	0.96172(5)	0.9330(3)	201(4)
Au1	0	0.07123(4)	0.6410(2)	245(3)
Au2	0	0.17904(4)	0.1412(2)	229(3)
Au3	0	0.26207(4)	0.9340(2)	262(4)
Au4	0	0.35112(3)	0.6848(2)	210(3)
Au5	0	0.39911(3)	0.1849(2)	226(3)
Au6	0	0.48762(3)	0.4344(2)	222(3)
Au7	0	0.57116(3)	0.2328(2)	257(3)
Au8	0	0.67868(4)	0.7340(2)	277(3)
Au9	0	0.76202(4)	0.9382(2)	259(4)
Au10	0	0.85087(3)	0.1898(3)	247(3)
Au11	0	0.89903(3)	0.6893(2)	228(3)
Au12	0	0.98763(4)	0.4380(2)	230(3)
In1	0	0.02103(7)	0.1413(4)	202(5)
In2	0	0.02176(7)	0.7327(4)	232(6)
In3	0	0.07458(7)	0.2517(4)	240(6)
In4	0	0.17539(6)	0.7530(4)	216(6)
In5	0	0.22834(6)	0.2295(4)	263(7)
In6	0	0.22884(7)	0.6401(4)	216(6)
In7	0	0.31428(6)	0.9617(4)	263(7)
In8	0	0.34894(7)	0.2992(4)	262(6)
In9	0	0.40070(7)	0.7982(4)	247(6)
In10	0	0.43593(7)	0.4613(4)	301(7)
In11	0	0.52115(7)	0.7285(4)	268(6)
In12	0	0.52145(7)	0.1421(4)	249(6)
In13	0	0.57443(7)	0.6202(4)	268(7)
In14	0	0.67524(7)	0.1202(5)	285(7)
In15	0	0.72821(7)	0.2316(4)	248(6)
In16	0	0.72873(6)	0.6393(4)	216(6)
In17	0	0.81430(6)	0.9107(4)	276(7)
In18	0	0.84922(6)	0.5793(4)	194(5)
In19	0	0.90106(5)	0.0773(4)	207(5)
In20	0	0.93558(7)	0.4087(4)	257(6)

Note. U_{eq} is defined as one-third of the trace of the orthogonalized U_{ij} tensor.

TABLE 4
Interatomic Distances (pm), Calculated with the Lattice Constants Taken from X-Ray Powder Data of $Ce_2Au_3In_5$

Ce1:	1	Au1	305.6(3)	Ce5:	1	Au7	307.1(3)	Au1:	1	In2	273.2(4)	Au7:	1	In12	274.2(4)
	2	Au11	324.6(2)		2	Au5	324.2(2)		2	In19	279.9(2)		2	In9	281.3(2)
	2	In18	327.1(3)		2	In8	325.7(3)		1	In3	288.9(3)		1	In13	287.4(4)
	2	Au10	333.5(2)		2	Au4	333.0(2)		1	Ce1	305.6(3)		1	Ce5	307.1(3)
	1	In3	338.9(4)		1	In14	337.4(4)		2	In20	307.8(2)		2	In10	309.8(2)
	1	In4	339.0(4)		1	In13	340.5(4)		2	Ce8	330.0(2)		2	Ce4	329.0(2)
	2	In19	346.1(3)		2	In9	347.3(3)								
	2	In20	358.7(3)		2	In10	360.9(3)	Au2:	1	In5	271.6(4)	Au8:	1	In16	276.7(4)
	1	Ce2	382.7(3)		1	Ce6	383.1(3)		2	In18	281.2(2)		2	In8	279.8(2)
	1	Ce2	384.5(2)		1	Ce6	384.6(3)		1	In4	288.1(4)		1	In14	286.6(4)
									1	Ce2	307.2(3)		1	Ce6	306.5(3)
Ce2:	1	Au2	307.2(3)	Ce6:	1	Au8	306.5(3)		2	In17	308.6(2)		2	In7	310.2(2)
	2	Au10	326.0(2)		2	Au4	323.2(2)		2	Ce7	330.3(2)		2	Ce3	326.9(2)
	2	In19	326.9(3)		2	In9	325.4(3)								
	2	Au11	332.1(2)		2	Au5	334.7(2)	Au3:	1	In7	280.0(4)	Au9:	1	In17	280.4(4)
	1	In3	337.7(4)		1	In14	337.9(5)		1	In6	280.9(4)		2	In6	280.9(2)
	1	In4	341.2(4)		1	In13	340.6(4)		2	In15	281.5(2)		1	In15	282.7(4)
	2	In18	344.4(2)		2	In8	348.5(3)		2	In16	282.2(2)		2	In5	284.0(2)
	2	In17	360.4(3)		2	In7	359.0(3)		1	In5	283.7(3)		1	In16	284.1(3)
	1	Ce1	382.7(3)		1	Ce5	383.1(3)		2	Ce7	354.2(2)		2	Ce3	356.7(3)
	1	Ce1	384.5(2)		1	Ce5	384.6(3)								
								Au4:	2	In14	276.2(2)	Au10:	2	In4	275.8(2)
Ce3:	2	Au8	326.9(2)	Ce7:	2	Au2	330.3(2)		1	In9	278.2(4)		1	In19	281.0(3)
	2	In16	332.2(3)		2	In6	330.6(3)		1	In7	284.4(4)		1	In17	284.6(4)
	2	In14	332.6(3)		2	In5	331.2(3)		1	In8	285.8(4)		1	In18	288.6(3)
	2	In15	332.7(3)		2	In4	332.5(3)		2	Ce6	323.2(2)		2	Ce2	326.0(2)
	1	In8	338.2(5)		1	In18	345.4(4)		2	Ce5	332.9(2)		2	Ce1	333.5(2)
	1	In6	353.8(4)		1	In16	351.1(4)								
	1	In5	355.8(4)		1	In15	352.4(4)	Au5:	2	In13	276.5(2)	Au11:	2	In3	276.0(2)
	2	Au9	356.7(3)		2	Au3	354.2(2)		1	In8	281.4(4)		1	In18	278.6(3)
	1	In7	376.0(4)		1	In17	380.6(4)		1	In10	284.1(4)		1	In20	285.3(3)
									1	In9	286.4(3)		1	In19	287.5(3)
Ce4:	2	Au7	329.1(2)	Ce8:	2	Au1	330.0(2)		2	Ce5	324.2(2)		2	Ce1	324.6(2)
	2	In11	329.8(3)		2	In1	330.6(3)		2	Ce6	334.7(2)		2	Ce2	332.2(2)
	2	In13	331.5(3)		2	In3	331.4(3)								
	2	In12	331.8(3)		2	In2	333.4(3)	Au6:	1	In10	277.2(4)	Au12:	1	In20	279.3(4)
	1	In9	342.8(5)		1	In19	341.6(4)		2	In11	282.1(2)		2	In1	280.9(2)
	1	In12	353.0(5)		1	In1	352.7(5)		1	In12	282.1(4)		2	In2	282.4(2)
	1	In11	353.2(5)		1	In2	353.7(4)		1	In11	282.1(4)		1	In1	283.2(4)
	2	Au6	356.8(3)		2	Au12	357.1(3)		2	In12	283.1(2)		1	In2	284.5(3)
	1	In10	379.1(4)		1	In20	378.9(4)		2	Ce4	356.8(3)		2	Ce8	357.1(3)
In1:	2	Au12	280.9(2)	In6:	2	Au9	280.9(2)	In11:	2	Au6	282.1(2)	In16:	1	Au8	276.7(4)
	1	Au12	283.2(4)		1	Au3	280.9(4)		1	Au6	282.1(4)		2	Au3	282.2(2)
	1	In3	297.8(5)		1	In4	297.8(5)		1	In13	296.0(5)		1	Au9	284.1(3)
	1	In2	302.6(4)		1	In5	304.1(4)		1	In12	306.3(4)		1	In15	301.9(4)
	2	Ce8	330.6(2)		2	Ce7	330.6(3)		2	Ce4	329.8(3)		2	Ce3	332.2(3)
	2	In2	333.3(4)		2	In15	333.9(2)		2	In12	331.8(5)		2	In5	333.7(2)
	1	Ce8	352.7(5)		1	Ce3	353.8(4)		1	Ce4	353.2(5)		1	Ce7	351.1(4)
	2	In20	371.0(4)		2	In17	369.1(4)		2	In10	369.5(4)		2	In7	352.6(4)
In2:	1	Au1	273.2(4)	In7:	1	Au3	280.0(4)	In12:	1	Au7	274.2(4)	In17:	1	Au9	280.4(4)
	2	Au12	282.4(2)		1	Au4	284.4(4)		1	Au6	282.1(4)		1	Au10	284.6(4)
	1	Au12	284.5(3)		2	Au8	310.2(2)		2	Au6	283.1(2)		1	In18	308.4(4)
	1	In1	302.6(4)		1	In8	311.1(4)		1	In11	306.3(4)		2	Au2	308.6(2)
	2	In1	333.3(4)		2	In14	348.1(4)		2	In11	331.8(5)		2	In4	348.4(3)
	2	Ce8	333.4(3)		2	In16	352.6(4)		2	Ce4	331.8(3)		2	In5	352.3(3)
	2	In20	350.9(4)		2	Ce6	359.0(3)		2	In10	352.2(4)		2	Ce2	360.4(3)
	1	Ce8	353.8(4)		2	In15	367.2(4)		1	Ce4	353.0(5)		2	In6	369.1(4)
					1	Ce3	376.0(4)						1	Ce7	380.6(4)

TABLE 4—*Continued*

In3:	2	Au11	276.0(2)						In13:	2	Au5	276.5(2)						
	1	Au1	288.9(3)	In8:	2	Au8	279.8(2)			1	Au7	287.4(4)	In18:	1	Au11	278.6(3)		
	1	In1	297.8(5)		1	Au5	281.4(4)			1	In11	296.0(5)		2	Au2	281.2(2)		
	2	Ce8	331.4(3)		1	Au4	285.8(4)			2	Ce4	331.5(3)		1	Au10	288.6(3)		
	1	Ce2	337.7(4)		1	In7	311.1(4)			1	Ce5	340.5(4)		1	In17	308.4(4)		
	1	Ce1	338.9(4)		2	Ce5	325.7(3)			1	Ce6	340.6(4)		2	Ce1	327.1(3)		
	2	In20	348.7(3)		1	Ce3	338.2(5)			2	In10	347.9(4)		2	Ce2	344.4(2)		
	2	In19	359.5(3)		2	Ce6	348.5(3)			2	In9	358.7(4)		1	Ce7	345.4(4)		
					2	In14	356.9(4)							2	In4	360.3(3)		
In4:	2	Au10	275.8(2)						In14:	2	Au4	276.2(2)						
	1	Au2	288.1(4)	In9:	1	Au4	278.2(4)			1	Au8	286.5(4)	In19:	2	Au1	279.9(2)		
	1	In6	297.8(5)		2	Au7	281.3(2)			1	In15	295.1(5)		1	Au10	281.0(3)		
	2	Ce7	332.6(3)		1	Au5	286.4(3)			2	Ce3	332.6(3)		1	Au11	287.5(3)		
	1	Ce1	339.0(4)		1	In10	312.6(4)			1	Ce5	337.4(4)		1	In20	307.1(4)		
	1	Ce2	341.2(4)		2	Ce6	325.3(3)			1	Ce6	337.9(5)		2	Ce2	326.9(3)		
	2	In17	348.4(3)		1	Ce4	342.8(5)			2	In7	348.1(4)		1	Ce8	341.6(4)		
	2	In18	360.3(3)		2	Ce5	347.3(3)			2	In8	356.9(4)		2	Ce1	346.1(3)		
					2	In13	358.7(4)							2	In3	359.5(3)		
In5:	1	Au2	271.6(4)						In15:	2	Au3	281.6(2)						
	1	Au3	283.6(3)	In10:	1	Au6	277.2(4)			1	Au9	282.7(4)	In20:	1	Au12	279.3(4)		
	2	Au9	284.0(2)		1	Au5	284.1(4)			1	In14	295.1(5)		1	Au11	285.3(3)		
	1	In6	304.1(4)		2	Au7	309.8(2)			1	In16	301.9(4)		1	In19	307.1(4)		
	2	Ce7	331.2(3)		1	In9	312.6(4)			2	Ce3	332.7(3)		2	Au1	307.8(2)		
	2	In16	333.7(2)		2	In13	347.9(4)			2	In6	333.9(2)		2	In3	348.7(3)		
	2	In17	352.3(3)		2	In12	352.2(4)			1	Ce7	352.4(4)		2	In2	351.0(4)		
	1	Ce3	355.8(4)		2	Ce5	360.9(3)			2	In7	367.1(4)		2	Ce1	358.7(3)		
					2	In11	369.5(4)							2	In1	371.0(4)		
					1	Ce4	379.1(4)							1	Ce8	378.9(4)		

Note. All distances within the first coordination sphere are listed.

sites were fully occupied within three standard deviations. In the final cycles the ideal occupancy parameters were assumed again.

The positional parameters and interatomic distances of the refinement are listed in Tables 3 and 4. Listings of the anisotropic displacement parameters and structure factor tables are available. (Details may be obtained from Fachinformationszentrum Karlsruhe, D-76344 Eggenstein-Leopoldshafen (Germany), by quoting the registry number CSD-410894.

Crystal Chemistry

The indium compounds $Ln_2Au_3In_5$ (Ln = Ce, Pr, Nd, Sm) crystallize with a new structure type which was determined from single crystal X-ray data for $Ce_2Au_3In_5$. The unit cell volume (Table 1) of these compounds decreases from the cerium to the samarium compound as expected from the lanthanoid contraction. As outlined in Fig. 2, the structure of $Ce_2Au_3In_5$ is built up from a complex three-dimensional $[Au_3In_5]$ polyanion, in which the cerium atoms are embedded.

The cerium atoms in $Ce_2Au_3In_5$ occupy eight crystallographically different sites, all on the Wyckoff site 2*a* of space group $Pmn2_1$ (No. 31). Although these cerium sites have slightly different coordinations (the distances are all distinctly different within the standard deviations), they can be grouped roughly into two categories. Four cerium sites have coordination number (CN) 15 with two cerium, five gold, and eight indium atoms in their coordination shell, while the others have CN14 with four gold and ten indium neighbors. Exclusively, the first group of cerium atoms has shorter Ce–Ce interactions ranging from 383 to 385 pm, but these Ce–Ce distances are already longer than those found in fcc cerium (24) where each cerium atom has twelve cerium neighbors at 365 pm. They are also well above the Hill limit (25) of 340 pm for *f* electron localization. The second group of cerium atoms in $Ce_2Au_3In_5$ has the closest cerium neighbors at distances of 465 pm. This Ce–Ce distance corresponds to the lattice parameter *a*.

The complex three-dimensional $[Au_3In_5]$ polyanion is composed of twelve crystallographically different gold atoms and twenty indium atoms. All gold atoms have CN 9. Three different groups of gold positions can be distinguished, four sites with 5 In + 4 Ce, three sites with 6 In + 3 Ce, and five sites with 7 In + 2 Ce. According to these different coordinations it seems to be clear that no higher symmetry is possible for the structure of $Ce_2Au_3In_5$. The various Au–In distances range from 272 to 310 pm. The shorter ones agree well with the sum of Pauling's single

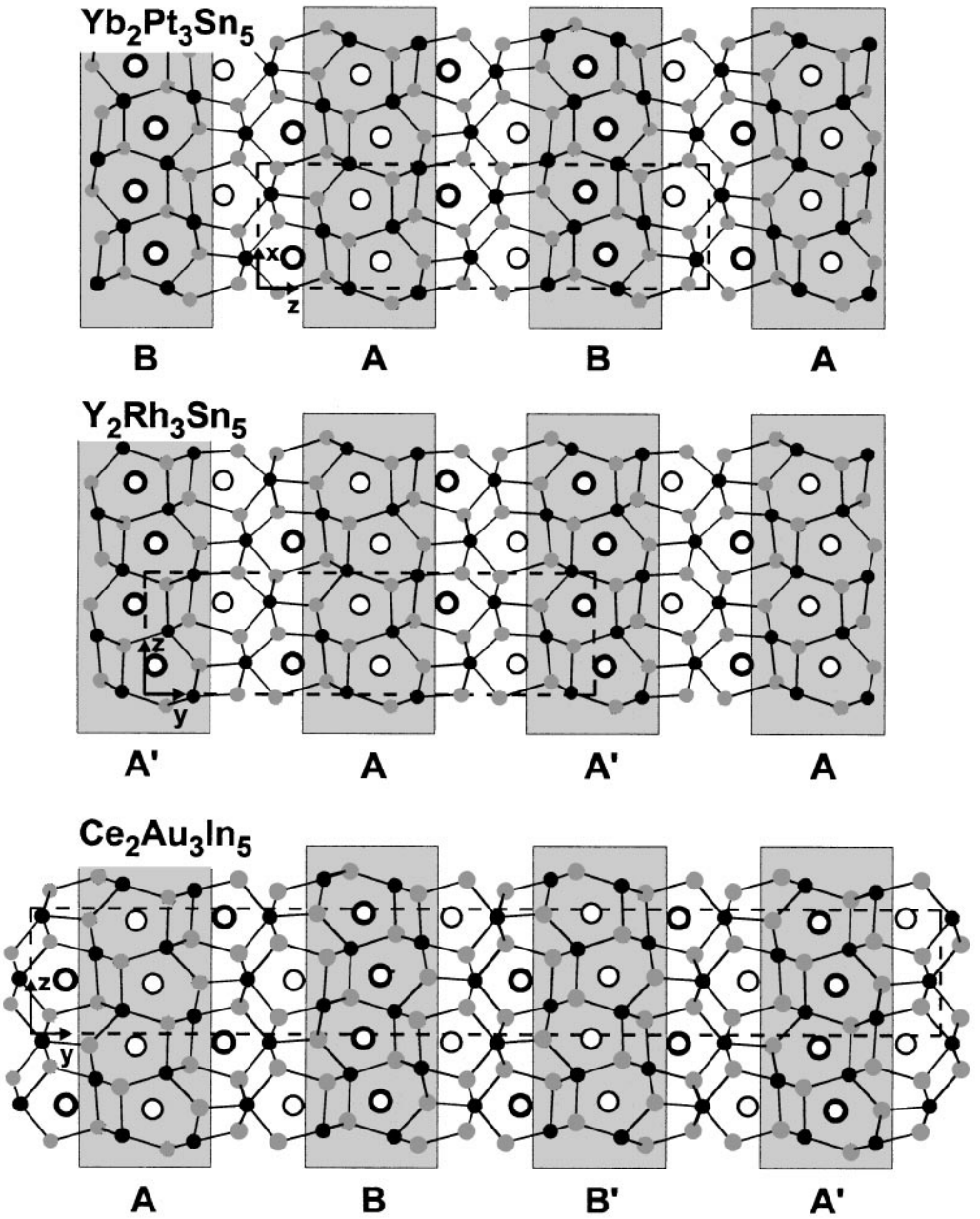

FIG. 2. Projections of the crystal structures of $Y_2Rh_3Sn_5$, $Yb_2Pt_3Sn_5$, and $Ce_2Au_3In_5$ along the short axes. The yttrium (ytterbium, cerium), rhodium (platinum, gold), and tin (indium) atoms are drawn as large open, black filled, and gray filled circles, respectively. Some relevant slabs are outlined. For details see text.

bond radii (26) of 273 pm for gold and indium, indicating strongly bonding Au–In interactions. Each gold atom has between 4 and 7 short Au–In contacts. Similar Au–In distances have recently also been observed in the compounds CaAuIn (280–289 pm) (27), GdAuIn (282–290 pm) (28), and $CaAuIn_2$ (282–285 pm) (29).

The short Au–Ce distances range from 306 to 307 pm. These are only slightly larger than the sum of Pauling's single bond radii (26) of 299 pm, but they are smaller than the sum of the metallic radii for CN12 (30) of 327 pm. This is in agreement with medium Au–Ce bonding. These interactions can certainly be expected, since the gold atoms are the more electronegative component of the polyanion (4.3 eV for Au and 3.1 eV for In according to Pearson (31)).

Within the polyanion we observe no Au–Au interactions. The monomeric structural units of the $[Au_3In_5]$ polyanions

are Au_2In_2 parallelograms which show a maximal separation of the gold atoms (in agreement with the higher electronegativity of Au). These Au_2In_2 parallelograms are condensed via common gold atoms or via Au–In bonds (Fig. 2) forming the complex polyanion. Such Au_2In_2 and Rh_2In_2 parallelograms occur also in the structures of $Ca_2Au_3In_4$ (32), $Sr_2Au_3In_4$ (33), CaRhIn (34), and $CaRhIn_2$ (34). The different concatenations of such T_2In_2 parallelograms allow a large variety of crystal structures with similar bonding characteristics.

The 20 crystallographically different indium sites in $Ce_2Au_3In_5$ have CN12–CN14. They have between 3 and 4 Au, 3 and 7 In, and 3 and 5 Ce neighbors. The In–In distances cover the large range from 295 to 371 pm; however, each indium atom has at least one short In–In contact. The In–In distances are shorter than the In–In distances in the tetragonal body-centered structure of elemental indium (a = 325.2 pm, c = 494.7 pm (24)), where each indium atom has four nearest neighbors at 325 pm and eight further neighbors at 338 pm with an average In–In distance of 334 pm.

According to the various short Au–In and In–In distances covalent Au–In and In–In bonding within the complex three-dimensional $[Au_3In_5]$ polyanion can be assumed. The cerium atoms as the least electronegative component have, in a first approximation, transferred their three valence electrons to the $[Au_3In_5]$ polyanion (see magnetic data discussed below). The formula can then be written as $[2Ce^{3+}]^{6+}[Au_3In_5]^{6-}$.

The structure of $Ce_2Au_3In_5$ has great similarities with the structures of the stannides $Y_2Rh_3Sn_5$ (15) and $Yb_2Pt_3Sn_5$ (16). Projections of these three structures along the short axes are presented in Fig. 2. At first sight, the polyanions $[Rh_3Sn_5]$, $[Pt_3Sn_5]$, and $[Au_3In_5]$ look quite similar; however, the three structure types crystallize with different space groups, $Y_2Rh_3Sn_5$ with space group $Cmc2_1$ (No. 36), $Yb_2Pt_3Sn_5$ with space group $Pnma$ (No. 62), and $Ce_2Au_3In_5$ with space group $Pmn2_1$ (No. 31). All of these structures have the common supergroup $Cmcm$ (No. 63), as outlined in the corresponding group–subgroup scheme (35, 36) in Fig. 1. A possible high-temperature phase with space group $Cmcm$ is unlikely to exist. Such a structure would require mixed gold/indium sites, which is questionable in view of the differences in chemical potential (and the electronegativities) of gold and indium.

The three structures consist of stacks of four basic building blocks, i.e., A and B and their counterparts A′ and B′ (Fig. 2). The latter are generated by a translation of 1/2, 1/2, 0 with respect to the subcell. The A′ and B building blocks are inverted with respect to each other, and they are translated by half a translation period within the projection direction with respect to the A block. Block B′ is shifted by half the translation period in the projection direction with respect to block B.

To summarize, for the composition $Ln_2T_3X_5$ three structure types, $Y_2Rh_3Sn_5$, $Yb_2Pt_3Sn_5$, and $Ce_2Au_3In_5$, are realized using different coloring of transition metal and indium (tin) atoms on the positions of the $[T_3X_5]$ polyanions. Nevertheless, the near-neighbor environments of the various atomic sites in the three structures are closely related, leading to the basic units labeled A, B, A′, and B′. The differences of the structures are based on the long-range order given by the stacking sequences A B, A B in $Yb_2Pt_3Sn_5$, A′ A, A′ A in $Y_2Rh_3Sn_5$, and A B B′ A′, A B B′ A′ in $Ce_2Au_3In_5$.

Magnetic Properties of $Ce_2Au_3In_5$

The temperature dependence of the inverse magnetic susceptibility of $Ce_2Au_3In_5$ is presented in Fig. 3. $Ce_2Au_3In_5$ shows Curie–Weiss behavior; however, a slight convex curvature is observed for the $1/\chi$ vs T plot, indicating a temperature-independent contribution. We have thus fit the data above 50 K with a modified Curie-Weiss expression $\chi = \chi_0 + C/(T - \Theta)$ resulting in a paramagnetic Curie temperature (Weiss constant) of $\Theta = -16(1)$ K, an experimental magnetic moment of 2.51(2) μ_B/Ce, and a temperature-independent contribution of $\chi_0 = 5.2(2) \times 10^{-9}$ m^3/mol. The experimental moment is close to the value 2.54 μ_B for the free Ce^{3+} ion (2), indicating trivalent cerium in $Ce_2Au_3In_5$. Down to 2 K no magnetic ordering could be detected. According to the negative Weiss constant we expect antiferromagnetic ordering at very low temperatures.

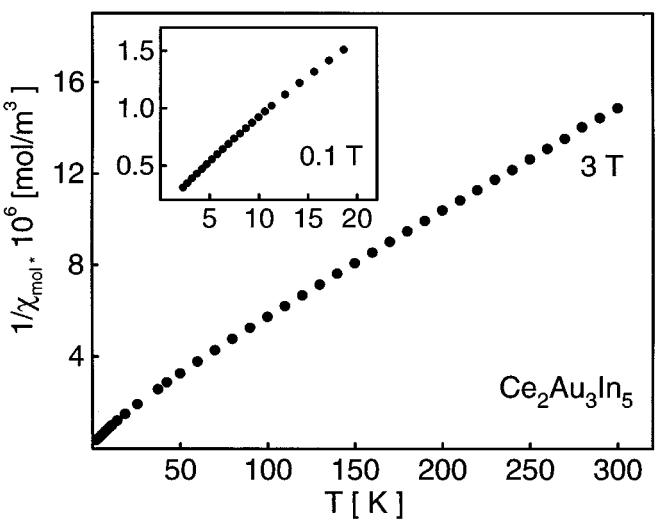

FIG. 3. Temperature dependence of the reciprocal magnetic susceptibility of $Ce_2Au_3In_5$ measured at a flux density of 3 T. The low-temperature behavior at 0.1 T is shown in the inset.

ACKNOWLEDGMENTS

We thank Prof. W. Jeitschko for his interest and support. We are also indebted to K. Wagner for the EDX analyses, to Dipl.-Chem. G. Kotzyba for the susceptibility measurement, and to Dr. W. Gerhartz (Degussa AG) for a generous gift of gold wire. Special thanks go to Prof. G. Erker, to Dr. R. Fröhlich (Münster), and to Dr. V. Enkelmann (Mainz) who let us use their diffractometers. This work was financially supported by the Fonds der Chemischen Industrie and by the Bennigsen-Foerder-Programm of the Ministerium für Wissenschaft und Forschung des Landes Nordrhein-Westfalen. Ya. V. Galadzhun is indebted to the DAAD for a research stipend.

REFERENCES

1. P. Villars and L. D. Calvert, "Pearson's Handbook of Crystallographic Data for Intermetallic Phases," 2nd ed. Am. Soc. for Metals, Materials Park, OH 44073, 1991. [And Desk Edition, 1997]
2. A. Szytuła and J. Leciejewicz, "Handbook of Crystal Structures and Magnetic Properties of Rare Earth Intermetallics." CRC Press, Boca Raton, FL, 1994.
3. Ya. M. Kalychak, *J. Alloys Compd.* **262–263,** 341 (1997).
4. Ya. M. Kalychak, E. I. Gladyshevskii, O. I. Bodak, O. V. Dmytrakh, and B. Ya. Kotur, *Sov. Phys. Crystallogr.* **30,** 344 (1985).
5. V. M. Baranyak, Ya. M. Kalychak, V. A. Bruskov, P. Yu. Zavalii, and O. V. Dmytrakh, *Sov. Phys. Crystallogr.* **33,** 353 (1988).
6. V. I. Zaremba, V. K. Belsky, Ya. M. Kalychak, V. K. Pecharsky, and E. I. Gladyshevskii, *Dopov. Akad. Nauk Ukr. RSR Ser. B*, 45 (1985).
7. Ya. M. Kalychak, V. M. Baranyak, and V. K. Belsky, *Dopov. Akad. Nauk Ukr. RSR Ser. B* 39 (1988).
8. V. M. Baranyak, Ya. M. Kalychak, and P. Yu. Zavalii, *Sov. Phys. Crystallogr.* **38,** 276 (1993).
9. R. Pöttgen, *J. Mater. Chem.* **5,** 769 (1995).
10. R. Pöttgen, R.-D. Hoffmann, R. K. Kremer, and W. Schnelle, *J. Solid State Chem.* **142,** 180 (1999).
11. L. V. Sysa, Ya. M. Kalychak, I. N. Stets', and Ya. V. Galadzhun, *Crystallogr. Rep.* **39,** 743 (1994).
12. L. V. Sysa, Ya. M. Kalychak, Ya. V. Galadzhun, V. I. Zaremba, L. G. Akselrud, and R. V. Skolozdra, *J. Alloys Compd.* **266,** 17 (1998).
13. Ya. V. Galadzhun and R. Pöttgen, *Z. Anorg. Allg. Chem.* **625,** 481 (1999).
14. Ya. V. Galadzhun, R.-D. Hoffmann, B. Künnen, G. Kotzyba, and R. Pöttgen, *Eur. J. Inorg. Chem.* 975 (1999).
15. M. Méot-Meyer, G. Venturini, B. Malaman, J. Steinmetz, and B. Roques, *Mater. Res. Bull.* **19,** 1181 (1984).
16. R. Pöttgen, A. Lang, R.-D. Hoffmann, B. Künnen, G. Kotzyba, R. Müllmann, B. D. Mosel, and C. Rosenhahn, *Z. Kristallogr.* **214,** 143 (1999).
17. R. Pöttgen, Th. Gulden, and A. Simon, *GIT Labor-Fachzeitschrift* **43,** 133 (1999).
18. K. Yvon, W. Jeitschko, and E. Parthé, *J. Appl. Crystallogr.* **10,** 73 (1977).
19. R. H. Blessing, *Acta Crystallogr.* **A51,** 33 (1995).
20. R. H. Blessing, *J. Appl. Crystallogr.* **30,** 421 (1997).
21. Z. Otwinowski and W. Minor, "Methods in Enzymology," Vol. 276, Macromolecular Crystallography, (C. W. Carter, Jr., and R. M. Sweet, Eds.), Part A, p. 307–326. Academic Press, San Diego, 1997.
22. G. M. Sheldrick, "SHELXS-97, Program for the Solution of Crystal Structures." University of Göttingen, Germany, 1997.
23. G. M. Sheldrick, "SHELXL-97, Program for Crystal Structure Refinement." University of Göttingen, Germany, 1997.
24. J. Donohue, "The Structures of the Elements." Wiley, New York, 1974.
25. H. H. Hill, *in* "Plutonium and Other Actinides" (W. N. Mines, Ed.), Nuclear Materials Series, Vol. 17, p. 2. AIME, New York, 1970.
26. L. Pauling, "The Nature of the Chemical Bond and The Structures of Molecules and Crystals." Cornell Univ. Press, Ithaca, NY, 1960.
27. D. Kußmann, R.-D. Hoffmann, and R. Pöttgen, *Z. Anorg. Allg. Chem.* **624,** 1727 (1998).
28. R. Pöttgen, G. Kotzyba, K. Latka, E. A. Görlich, and R. Dronskowski, *J. Solid State Chem.* **141,** 352 (1998).
29. R.-D. Hoffmann, R. Pöttgen, G. A. Landrum, R. Dronskowski, B. Künnen, and G. Kotzyba, *Z. Anorg. Allg. Chem.* **625,** 789 (1999).
30. E. Teatum, K. A. Gschneidner, Jr., and J. Waber, Report LA-2345, U.S. Department of Commerce, Washington, DC, 1960.
31. R. G. Pearson, *Inorg. Chem.* **27,** 734 (1988).
32. R.-D. Hoffmann and R. Pöttgen, *Z. Anorg. Allg. Chem.* **625,** 994 (1999).
33. R.-D. Hoffmann, R. Pöttgen, C. Rosenhahn, B. D. Mosel, B. Künnen, and G. Kotzyba, *J. Solid State Chem.* **145,** 283 (1999).
34. R.-D. Hoffmann and R. Pöttgen, *Z. Anorg. Allg. Chem.*, in press.
35. H. Bärnighausen, *Commun. Math. Chem.* **9,** 139 (1980).
36. H. Bärnighausen and U. Müller, "Symmetriebeziehungen zwischen den Raumgruppen als Hilfsmittel zur straffen Darstellung von Strukturzusammenhängen in der Kristallchemie." Universität Karlsruhe and Universität-Gh Kassel, Germany, 1996.